JOURNAL OF SOLID STATE CHEMISTRY 102, 115–125 (1993)

Structures of the Stuffed Tridymite Derivatives, BaMSiO$_4$ (M = Co, Zn, Mg)

B. LIU AND J. BARBIER

Department of Chemistry, McMaster University, Hamilton, Ontario, Canada L8S 4M1

Received February 25, 1992; in revised form June 18, 1992; accepted June 24, 1992

The crystal structures of the compounds BaMSiO$_4$ (M = Co, Mg, Zn) have been refined by using single-crystal X-ray data (M = Co) and powder neutron data (M = Mg, Zn). The three compounds are isostructural Ba-stuffed derivatives of tridymite (SiO$_2$) and crystallize with a ($\sqrt{3} \times A$, C) superstructure of hexagonal (A, C) kalsilite (KAlSiO$_4$). A clear correlation exists between the degree of collapse of the fully ordered tetrahedral framework and the size difference between the M and Si atoms.

1. Introduction

The compounds BaMSiO$_4$ (M = Co, Mg, Zn) belong to the large structural family of stuffed tridymite (SiO$_2$) derivatives (*1*). The latter are obtained by partially replacing Si^{4+} ions with other tetrahedrally coordinated ions of lower valence, such as Mg^{2+} and Zn^{2+}, and by stuffing large ions, such as Ba^{2+}, into the cavities of the tetrahedral framework to maintain charge balance.

The study of these tridymite derivatives is of interest in view of their complex polymorphism and their relationship to the mineral kalsilite (KAlSiO$_4$), which itself has been the subject of numerous studies [e.g., (*2–6*)]. In particular, the effect of atomic substitution on the topology of the tetrahedral framework has recently been investigated in a number of systems, such as MAl$_2$O$_4$ (M = Ca, Sr, Ba) (*7–12*), (Na,K)AlGeO$_4$ (*13–15*), and (Na,K)GaXO$_4$ (X = Si, Ge) (*16*). The original study (*17*) of the Ba-substituted compounds BaAl$_2$O$_4$, BaMgSiO$_4$, BaZnSiO$_4$, and BaZnGeO$_4$ had reported them to crystallize with small, hexagonal unit cells (with $A \approx 5.25$ Å and $C \approx 8.75$ Å), suggesting that they were simply isostructural with kalsilite. However, later studies established the existence of a ($2 \times A$, C) superstructure for BaAl$_2$O$_4$ (*8*) and a temperature-dependent ($\sqrt{3} \times$ A, $4 \times$ C) superstructure for BaZnGeO$_4$ (*18, 19*). For the latter, only an approximate structure of the room temperature phase could be determined by single-crystal X-ray diffraction by neglecting the very weak and incommensurate $4 \times C$ superstructure (*20*).

The present paper reports reports on the reinvestigation of the BaMgSiO$_4$ and BaZnSiO$_4$ compounds using powder X-ray and neutron diffraction and the discovery of a new isostructural compound, BaCoSiO$_4$. The structure of the latter has been determined by using single-crystal X-ray diffraction.

2. Powder Syntheses and Characterization

The syntheses of the three compounds BaZnSiO$_4$, BaMgSiO$_4$, and BaCoSiO$_4$ were

0022-4596/93 $5.00

carried out by high-temperature sintering of stoichiometric mixtures of $Ba(CH_3COO)_2$, ZnO (first dried at 900°C), MgO, $CoCO_3$, and silica gel (80.04 wt% SiO_2, as determined by TGA). The powder mixtures were pressed into pellets, heated up to 700–900°C to decompose the acetate or carbonate, remixed, and fired at 1300°C for $BaZnSiO_4$, 1560°C for $BaMgSiO_4$, and 1250°C for $BaCoSiO_4$ for about 48–72 hr with intermediate remixing. Finally the samples were quenched in air and ground into fine powders for X-ray and neutron diffraction experiments. Both the $BaZnSiO_4$ and $BaMgSiO_4$ powders were white, whereas the $BaCoSiO_4$ was deep blue as expected for a compound containing tetrahedral Co^{2+} ions. The blue color of the Co compound was observed to turn slightly darker after annealing at temperatures below about 1100°C, and this color change was found to be associated with the decomposition of $BaCoSiO_4$ into a mixture of CoO and $Ba_2CoSi_2O_7$. The latter compound is probably isostructural with $Ba_2CuSi_2O_7$ (*21*). No such decomposition was observed for the Zn or Mg compounds.

In all cases, the nature of the final products was analyzed by powder X-ray diffraction using a Guinier–Hägg camera ($CuK\alpha_1$ radiation, $\lambda = 1.540598$ Å) and silicon powder as an internal standard. The films were read with a computer-controlled LS-20 digital scanner, and the diffraction data were then used to determine and refine the unit-cell parameters by means of a local least-squares refinement program. The powder X-ray diffraction patterns of all three compounds were indexed on a similar ($\sqrt{3} \times A$, C) hexagonal unit cell, a superstructure of the basic (A, C) kalsilite cell required by the presence of a few weak reflections of the type $\{hkl, h - k \neq 3n\}$. The refined unit-cell parameters are shown in Table I. Interestingly, the variations in cell parameters and cell volume do not correlate with the practically identical Mg–O, Zn–O, and Co–O bond lengths predicted from ionic radii (1.95, 1.96, and 1.98 Å for tetrahedrally coordinated atoms) (*22*) (cf. Section 5).

TABLE I

HEXAGONAL UNIT-CELL PARAMETERS (Å) AND VOLUMES (Å^3) FOR THE $BaMSiO_4$ (M = Co, Mg, Zn) COMPOUNDS

	a	c	V
$BaCoSiO_4$			
Powder X-ray	9.1231(6)	8.6818(10)	625.79(9)
Single crystal X-ray	9.126(2)	8.683(4)	626.3(5)
$BaZnSiO_4$			
Powder X-ray	9.0955(5)	8.7251(9)	625.11(7)
Powder neutron	9.0850(9)	8.7147(11)	622.9(2)
$BaMgSiO_4$			
Powder X-ray	9.1226(7)	8.7496(15)	630.6(1)
Powder neutron	9.1118(6)	8.7371(8)	628.2(2)

All three compounds were also examined by electron diffraction/microscopy using a Philips CM-12 transmission electron microscope operating at 120 kV and equipped with a double-tilt goniometer stage. The electron diffraction patterns confirmed the presence of a $\sqrt{3} \times A$ superstructure in the basal plane of the hexagonal cell (Fig. 1a) and also showed the absence of a superstructure along the c axis (Fig. 1b). These results therefore indicate that the compounds $BaMgSiO_4$, $BaZnSiO_4$, and $BaCoSiO_4$ adopt a structure more complex than the simple kalsilite structure and that they are structurally closely related to the room temperature form of $BaZnGeO_4$ (*20*).

3. Powder Neutron Refinement of the $BaMgSiO_4$ and $BaZnSiO_4$ Structures

Neutron powder diffraction data for $BaMgSiO_4$ and $BaZnSiO_4$ were collected at the McMaster Nuclear Reactor. Powder samples, of about 8 g each, were loaded in a thin-walled vanadium can and neutrons, with a wavelength of 1.3907 Å, were obtained from a [200] copper monochromator. The diffraction data were recorded at room temperature over the angular range $10° <$

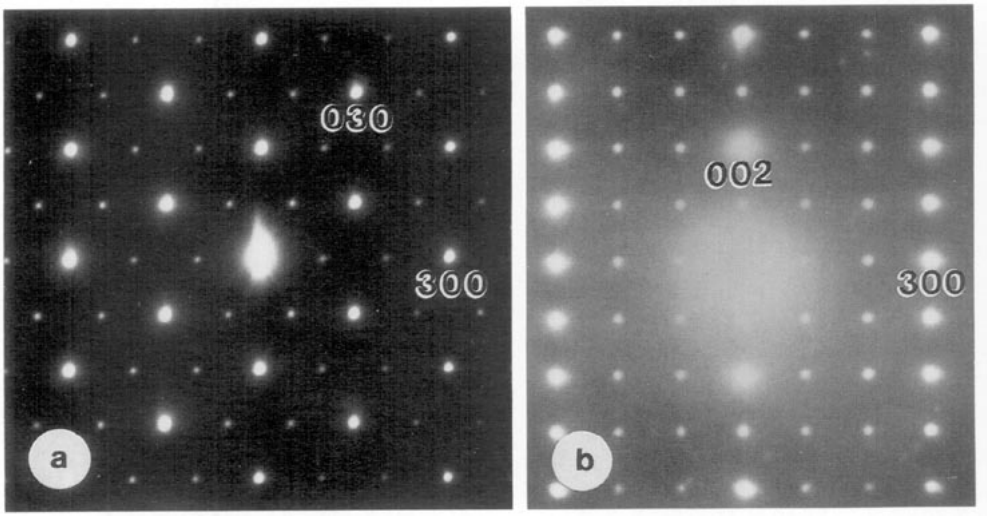

FIG. 1. (a) [001] and (b) [010] zone-axis electron diffraction patterns of $BaMSiO_4$ (M = Co, Mg, Zn). Note the $\sqrt{3}$ superstructure in the basal plane of the hexagonal unit cell and the absence of superstructure along the c axis. The {00l, l odd} reflections (forbidden in the $P6_3$ space group) appear by double diffraction.

$2\theta < 92°$ at four different settings of the position-sensitive detector. After correction of the raw data for detector geometry (*23*), the profile refinement was carried out with a local version of the Rietveld program. The following scattering lengths (10^{-12} cm) were used: Ba (0.525), Mg (0.5357), Zn (0.568), Si (0.4149), O (0.5805) (*24*).

The refinements of the $BaMgSiO_4$ and $BaZnSiO_4$ structures were performed in a similar way, starting with the cell parameters determined by powder X-ray diffraction (cf. Table I) and the atomic positions determined in the $P6_3$ space group for the isostructural subcell of the $BaZnGeO_4$ compound (*20*). The Ba atoms were positioned on the 2*a* and 2*b* sites, and the Si, O, Mg, or Zn atoms occupied three sets of general 6*c* sites.

The structural parameters allowed to vary during the refinements included the cell parameters, the atomic coordinates, and the isotropic temperature factors. A complete ordering of the Si/Mg and Si/Zn atoms was assumed initially and later confirmed by the final refinements and bond length data. Due to strong correlations between variables, it was found necessary to apply constraints on the temperature factors of similar atoms. The refinements then converged smoothly to the following agreement indices: weighted profile index R_{wp} = 0.042/0.054, nuclear index R_n = 0.026/0.046, and expected index R_e = 0.026/0.027 for $BaMgSiO_4/BaZnSiO_4$, respectively. The cell parameters obtained are very close to those refined from powder X-ray diffraction data (cf. Table I), the small difference (by a constant ratio of 0.999) probably reflecting a slight error in the wavelength calibration of the neutron powder diffractometer. The final positional and thermal parameters are listed in Table II and the calculated, observed, and difference profiles are shown in Fig. 2 for the case of $BaMgSiO_4$. Selected bond lengths, bond angles, and bond valence sums (*25*) are listed in Table III. It should be noted that the larger e.s.d.'s for the z coordinates in Table II are a result of the strong correlations noted earlier and that

TABLE II

FINAL ATOMIC POSITIONS AND ISOTROPIC TEMPERATURE FACTORS FOR THE NEUTRON POWDER REFINEMENTS OF $BaMgSiO_4$ AND $BaZnSiO_4$

Atom	Site	x	y	z	$B(Å^2)^a$
			$BaMgSiO_4$		
Ba(1)	2*a*	0	0	$\frac{1}{4}^b$	0.91(8)[c]
Ba(2)	2*b*	$\frac{1}{3}$	$\frac{2}{3}$	0.236(3)	0.91(8)
Ba(3)	2*b*	$\frac{2}{3}$	$\frac{1}{3}$	0.231(3)	0.91(8)
Si	6*c*	0.653(2)	−0.017(2)	0.435(3)	0.50(7)
Mg	6*c*	0.6738(12)	0.668(2)	0.539(3)	0.50(7)
O(1)	6*c*	0.762(1)	0.9025(12)	0.516(3)	1.17(6)
O(2)	6*c*	0.4681(1)	0.8980(12)	0.498(3)	1.17(6)
O(3)	6*c*	0.767(1)	0.1918(12)	0.456(3)	1.17(6)
O(4)	6*c*	0.7090(9)	0.6581(12)	0.751(3)	2.2(2)
			$BaZnSiO_4$		
Ba(1)	2*a*	0	0	$\frac{1}{4}^b$	1.1(1)
Ba(2)	2*b*	$\frac{1}{3}$	$\frac{2}{3}$	0.232(4)	1.1(1)
Ba(3)	2*b*	$\frac{2}{3}$	$\frac{1}{3}$	0.233(3)	1.1(1)
Si	6*c*	0.649(2)	−0.021(2)	0.434(4)	0.31(8)
Zn	6*c*	0.670(2)	0.664(2)	0.538(3)	0.31(8)
O(1)	6*c*	0.762(2)	0.902(2)	0.519(4)	1.32(8)
O(2)	6*c*	0.468(2)	0.897(2)	0.499(4)	1.32(8)
O(3)	6*c*	0.764(2)	0.193(2)	0.455(3)	1.32(8)
O(4)	6*c*	0.710(2)	0.660(2)	0.751(4)	4.1(3)

[a] The temperature factors of the Ba atoms, tetrahedral atoms, and O(1–3) atoms were constrained to be equal during the refinements.

[b] Used to fix the origin in the $P6_3$ space group.

[c] The estimated standard deviations on the last digits are given in parentheses.

the larger unconstrained temperature factors of the O(4) atoms suggest positional disorder similar to that observed in, for instance, $KAlSiO_4$ (*2*) and $BaZnGeO_4$ (*20*).

4. Single-Crystal X-Ray Refinement of the $BaCoSiO_4$ Structure

Single crystals of $BaCoSiO_4$ were obtained by a melt growth technique. A 10-g stoichiometric mixture of barium acetate, cobalt carbonate, and silica gel was finely ground and pressed into a pellet. The pellet was first fired at 700–900°C to decompose the acetate and carbonate, then remixed and melted in a platinum crucible at 1350°C. The sample was soaked at this temperature for 2 hr, cooled down to 1150°C at a rate of 2°/hr, and finally quenched from this temperature to prevent the decomposition reaction of $BaCoSiO_4$ (cf. Section 2). The products consisted of a mixture of deep blue $BaCoSiO_4$ crystals plus colorless crystals, indicating an incongruent melting reaction for the barium compound.

The intensity data were collected from a crystal with dimensions of 0.30 × 0.80 × 0.10 mm^3 on a Siemens R3m/v diffractometer using graphite-monochromatized Ag$K\alpha$ radiation. All crystal data, data collection parameters, and results of analysis are listed in Table IV. The unit-cell constants, determined from 25 single reflections, are in close agreement with those refined from powder diffraction data (cf. Table I). The structure was solved in the $P6_3$ space

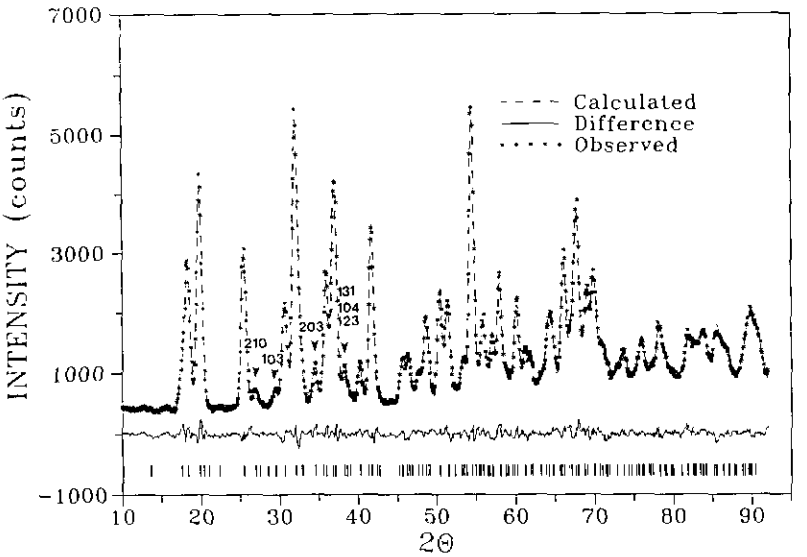

FIG. 2. Observed (*), calculated (---), and difference (bottom) powder neutron diffraction profiles for $BaMgSiO_4$. The (|) signs indicate the Bragg peak positions. A few well-resolved superstructure reflections are indicated by down arrowheads.

group by direct methods and successive Fourier syntheses. To be consistent with the $BaMgSiO_4$ and $BaZnSiO_4$ structures, the Ba(1) atom was chosen to fix the origin. An ordered arrangement of the tetrahedral Co and Si atoms was also assumed initially and later confirmed during the refinement. Using 1062 observed reflections ($F > 6\sigma(F)$), a full-matrix least-squares refinement was carried out with anisotropic temperature factors for all atoms, converging to final agreement indices $R = 0.035$ and $R_w = 0.042$. The final atomic positions and equivalent isotropic displacement parameters are listed in Table V and the anisotropic thermal parameters are shown in Table VI. Selected bond lengths, bond angles, and associated bond valences (25) are given in Table VII.

The single-crystal X-ray refinement of the $BaCoSiO_4$ structure yields a better precision (by about a factor of 10) for the atomic coordinates and bond distances than the neutron powder refinements of the $BaMgSiO_4$ and $BaZnSiO_4$ structures. The three compounds are, nevertheless, clearly isostructural with very similar atomic positions and environments. Note in particular that the temperature factor of the O(4) atom in the Co compound is again larger than those of the other oxygen atoms, suggesting some structural disorder which, however, has not been investigated further.

5. Description of the Structures and Discussion

Except for minor shifts in atomic positions (cf. Tables II and V), the structures of the three compounds BaMSiO$_4$ (M = Co, Mg, Zn) are identical and only the more accurately determined structure of $BaCoSiO_4$ is shown in Fig. 3, viewed along the c axis of the hexagonal unit cell. As in the structure of kalsilite, $KAlSiO_4$ (2), the tetrahedral framework of the $BaCoSiO_4$ structure consists of six-membered rings of corner-shared tetrahedra pointing alternately up and down. All rings are identical

TABLE III

SELECTED BOND LENGTHS[a] (Å), BOND ANGLES[a] (°), AND BOND VALENCE SUMS (Σ) IN THE $BaMgSiO_4$ AND $BaZnSiO_4$ STRUCTURES

$BaMgSiO_4$		$BaZnSiO_4$	
Ba(1)–O(1) × 3	2.78(2)	Ba(1)–O(1) × 3	2.78(3)
Ba(1)–O(1) × 3	2.99(2)	Ba(1)–O(1) × 3	2.98(3)
Ba(1)–O(4) × 3	2.91(1)	Ba(1)–O(4) × 3	2.88(2)
Mean	2.89	Mean	2.88
Σ	1.87	Σ	1.91
Ba(2)–O(2) × 3	2.93(2)	Ba(2)–O(2) × 3	2.96(4)
Ba(2)–O(3) × 3	3.11(2)	Ba(2)–O(3) × 3	3.06(4)
Ba(2)–O(4) × 3	2.789(9)	Ba(2)–O(4) × 3	2.79(1)
Mean	2.94	Mean	2.94
Σ	1.62	Σ	1.62
Ba(3)–O(2) × 3	2.74(2)	Ba(3)–O(2) × 3	2.73(3)
Ba(3)–O(3) × 3	2.94(2)	Ba(3)–O(3) × 3	2.71(3)
Mean	2.74	Mean	2.72
Σ	1.75	Σ	1.85
Si–O(1)	1.62(2)	Si–O(1)	1.67(2)
Si–O(2)	1.60(2)	Si–O(2)	1.53(2)
Si–O(3)	1.66(1)	Si–O(3)	1.70(2)
Si–O(4)	1.64(1)	Si–O(4)	1.63(2)
Mean	1.63	Mean	1.63
Σ	3.94	Σ	3.97
O–Si–O	105.4–113.5	O–Si–O	103.9–114.8
Mg–O(1)	1.88(2)	Zn–O(1)	1.90(2)
Mg–O(2)	1.96(1)	Zn–O(2)	1.93(2)
Mg–O(3)	1.95(1)	Zn–O(3)	1.95(1)
Mg–O(4)	1.87(1)	Zn–O(4)	1.89(2)
Mean	1.92	Mean	1.92
Σ	2.21	Σ	2.25
O–Mg–O	100–117.2	O–Zn–O	98.2–116.2

[a] Selected bond lengths and angles have been calculated based on the cell dimensions refined from powder neutron data (cf. Table I).

[b] The estimated standard deviations on the last digits are given in parentheses.

with an almost triangular shape and are stacked along the *c* direction, joined via the O(4) oxygen atoms in a staggered configuration, again similar to that found in kalsilite.

As indicated by the structural refinements and the bond length data (cf. Tables III and VII), the tetrahedral *M* (= Co, Mg, Zn) and Si atoms are completely ordered, and, in the $BaCoSiO_4$ structure shown in Fig. 3, all the large CoO_4 tetrahedra point up while all the small SiO_4 tetrahedra point down. Such a fully ordered arrangement could be expected in spite of the high temperatures used for the powder syntheses and the single-crystal growth (1150–1560°C) because of the large differences in formal ionic valences (M^{2+} vs Si^{4+}) and in bond lengths (1.92–1.96 Å for *M*–O vs 1.63 Å for Si–O).

TABLE IV

SUMMARY OF SINGLE-CRYSTAL DATA, INTENSITY MEASUREMENTS, AND STRUCTURE REFINEMENT PARAMETERS FOR $BaCoSiO_4$

	Crystal data
Crystal system	Hexagonal
Space group	$P6_3$
Unit-cell dimensions	a = 9.126(2) Å, c = 8.683(4) Å
Volume	626.3(5) Å^3
Z	6
Crystal size	0.30 × 0.08 × 0.10 mm^3
Formula weight	288.4
Density (calc.)	4.587 mg/m^3
Absorption coefficient	13.508 mm^{-1}
F(000)	774
	Data collection
Diffractomer	Siemens R3m/V
Radiation	Ag$K\alpha$ (λ = 0.56086 Å)
Temperature (K)	300
Monochromator	High oriented graphite crystal
2θ range	5.0 to 65.0°
Scan type	$2\theta - \theta$
Scan speed	Variable, 1.50 to 14.65°/min in ω
Scan range (ω)	1.20° plus $K\alpha$ separation
Standard reflections	2 2 2, 2 2 −2, −3 6 0, measured every 100 reflections
Index range	$-17 \le h \le 15$, $0 \le k \le 17$, $0 \le l \le 16$
Reflections collected	5080
Independent reflections	1631 (R_{int} = 4.75%)
Observed reflections	1062 ($F > 6.0\sigma(F)$)
Absorption correction	Semiempirical
Min/max transmission	0.2777/0.5233
	Solution and refinement
System	Siemens SHELXTL PLUS (VMS)
Solution	Direct methods and Fourier difference
Refinement method	Full-matrix least-squares
Quantity minimized	$\Sigma w(F_o - F_c)^2$
Absolute structure	N/A
Extinction correction	χ = 0.00074(8), where $F^* = F[1 + 0.002 \times F^2/\sin(2\theta)]^{-1/4}$
Weighting scheme	$w^{-1} = \sigma^2(F) + 0.0008F^2$
Number of parameters refined	64
Final R indices (observed data)	R = 3.48%, wR = 4.15%
R indices (all data)	R = 6.05%, wR = 5.83%
Goodness-of-fit	0.93
Largest and mean Δ/σ	0.012, 0.004
Data-to-parameter ratio	16.6:1
Largest difference peak	2.89 e Å^{-3}
Largest difference hole	−4.04 e Å^{-3}

A similar tetrahedral ordering has also been reported for the isostructural room temperature phase of $BaZnGeO_4$ (*20*).

All three crystallographically independent Ba atoms of the $BaMSiO_4$ structures are located on the threefold axes with, however, different coordination environments: in $BaCoSiO_4$ for example, Ba(1) is nine-coordinated [six O(1)'s plus three O(4)'s at an average distance of 2.89 Å], Ba(2) is also

TABLE V

ATOMIC COORDINATES AND EQUIVALENT ISOTROPIC DISPLACEMENT COEFFICIENTS (Å^2 × 10^3) FOR THE SINGLE-CRYSTAL X-RAY REFINEMENT OF $BaCoSiO_4$

Atom	Site	x	y	z	U_{eq}[a]
Ba(1)	2*a*	0	0	$\frac{1}{4}$[b]	12(1)[c]
Ba(2)	2*b*	$\frac{1}{3}$	$\frac{2}{3}$	0.2197(1)	14(1)
Ba(3)	2*b*	$\frac{2}{3}$	$\frac{1}{3}$	0.2185(1)	16(1)
Si	6*c*	0.6588(2)	−0.0118(2)	0.4303(3)	10(1)
Co	6*c*	0.6823(1)	0.6711(1)	0.5322(2)	12(1)
O(1)	6*c*	0.7635(6)	0.9139(6)	0.5211(9)	21(2)
O(2)	6*c*	0.4645(7)	0.9050(8)	0.4889(8)	21(2)
O(3)	6*c*	0.7612(6)	0.1950(6)	0.4459(3)	17(2)
O(4)	6*c*	0.7223(8)	0.6534(9)	0.7527(8)	30(2)

[a] $U_{eq} = \frac{1}{3}(U_{11} + U_{22} + U_{33})$

[b] Used to fix the origin in the $P6_3$ space group.

[c] The estimated standard deviations on the last digits are given in parentheses.

nine-coordinated [three O(2)'s, three O(3)'s, and three O(4)'s at an average distance of 2.92 Å], but Ba(3) is only six-coordinated [three O(2)'s plus three O(3)'s at a shorter average distance of 2.73 Å] (cf. Table VII). It can be seen in Fig. 3 and Table VII that the lower coordination of the third Ba atom arises from the displacement of the O(4) atom (at height 25) away from Ba(3) and toward Ba(1) and Ba(2). [Note that the Ba(2) and Ba(3) positions alternate at heights 25 and 75 on the threefold axes so that the O(4) atom at height 75 is also displaced away from Ba(3).] It is clear also from Fig. 3 that this shift of the O(4) atom from its ideal position at $(\frac{1}{3}, \frac{1}{3}, \frac{1}{4})$ or $(\frac{2}{3}, \frac{2}{3}, \frac{3}{4})$ is the main factor behind the formation of the $\sqrt{3} \times A$ superstructure in the basal plane of the $BaMSiO_4$ unit cells. This atom shift is similar to that commonly observed in the structures of the kalsilite–nepheline series, $(K,Na)AlSiO_4$ [e.g., (26)], and appears necessary to (i) release the strain in the Co–O(4)–Si bond angle which decreases to 148.6(5)° and (ii) accommodate the bonding requirements of all three Ba atoms which, in spite of different

TABLE VI

ANISOTROPIC THERMAL PARAMETERS[a] (Å^2 × 10^3) OF $BaCoSiO_4$

	U_{11}	U_{22}	U_{33}	U_{12}	U_{13}	U_{23}
Ba(1)	14(1)	14(1)	9(1)	7(1)	0	0
Ba(2)	15(1)	15(1)	12(1)	7(1)	0	0
Ba(3)	20(1)	20(1)	8(1)	10(1)	0	0
Si	10(1)	10(1)	9(1)	4(1)	2(1)	3(1)
Co	13(1)	12(1)	11(1)	7(1)	−1(1)	−2(1)
O(1)	20(2)	14(2)	31(2)	0(2)	−14(3)	0(3)
O(2)	15(2)	18(2)	31(4)	9(2)	13(2)	9(2)
O(3)	13(2)	14(2)	24(3)	5(2)	−7(2)	−1(2)
O(4)	37(3)	36(3)	10(2)	11(3)	3(2)	−5(2)

[a] The anisotropic displacement factor exponent takes the form $-2\pi^2(h^2a^{*2}U_{11} + \ldots + 2hka^*b^*U_{12})$.

TABLE VII

SELECTED BOND LENGTHS[a] (Å), BOND ANGLES[a] (°), AND BOND VALENCES (s) IN THE $BaCoSiO_4$ STRUCTURE

		l	s
Ba(1)–O(1) × 3		2.744(7)[b]	0.289(×3)
Ba(1)–O(1) × 3		3.020(8)	0.137(×3)
Ba(1)–O(4) × 3		2.900(9)	0.190(×3)
	Mean	2.888	Σ 1.85
Ba(2)–O(2) × 3		3.004(6)	0.143(×3)
Ba(2)–O(3) × 3		3.013(7)	0.140(×3)
Ba(2)–O(4) × 3		2.718(9)	0.310(×3)
	Mean	2.912	Σ 1.78
Ba(3)–O(2)×3		2.745(5)	0.288(×3)
Ba(3)–O(3)×3		2.706(6)	0.321(×3)
{Ba(3)–O(4)×3		3.629(9)}[c]	
	Mean	2.726	Σ 1.83
Si–O(1)		1.626(8)	0.995
Si–O(2)		1.623(6)	1.003
Si–O(3)		1.639(5)	0.960
Si–O(4)		1.620(7)	1.011
	Mean	1.627	Σ 3.97
O–Si–O		104.9–112.6	
Co–O(1)		1.956(5)	0.490
Co–O(2)		1.952(6)	0.495
Co–O(3)		1.951(7)	0.497
Co–O(4)		1.971(7)	0.470
	Mean	1.957	Σ 1.95
O–Co–O		99.1–123.5	

[a] Selected bond lengths and angles have been calculated based on the cell dimensions from the single-crystal X-ray refinement (cf. Table I).

[b] The estimated standard deviations on the last digits are given in parentheses.

[c] The very long bond was excluded when the mean bond length and bond valence sum were calculated.

environments, end up with similar bond valence sums (cf. Table VII). (The small variations in bond valence sums observed in the cases of $BaMgSiO_4$ and $BaZnSiO_4$ in Table III are probably the result of less accurate refinements using powder data.) It is worth noting, however, that the bond valence sums around the Ba atoms in all three compounds are lower than expected and indicate that the Ba–O bonds are stretched in the room temperature structures (i.e., the Ba atoms are somewhat too small relative to the size of the framework cavities). This result is consistent with the observation that, at least for $BaCoSiO_4$, the structure is stable at high temperature only.

The displacement of the O(4) atom also corresponds to the collapse of the tetrahedral framework around the barium atoms, involving the tilting of the CoO_4 and SiO_4 tetrahedra around horizontal axes approximately parallel to the [110] direction or equivalent directions (cf. Fig. 3). This tilting of the tetrahedra relative to the (001) basal plane together with their rotation around their pseudo-threefold axis parallel to the c direction is a common feature of stuffed tridymite derivative structures [e.g., (*10*, *11*). The degree of framework collapse in the $BaMSiO_4$ structures can be qualitatively estimated from the difference (Δz) between the z coordinates of the O(1) and O(3) atoms: Δz is equal to 0.060(6), 0.064(6), and 0.075(1) for $BaMgSiO_4$, $BaZnSiO_4$, and $BaCoSiO_4$, respectively (cf. Tables II and V), indicating an increasing degree of tetrahedral tilting. The same effect is also apparent from the comparison of the M–O(4)–Si bond angles which are equal to 157.9(13), 156.1(16), and

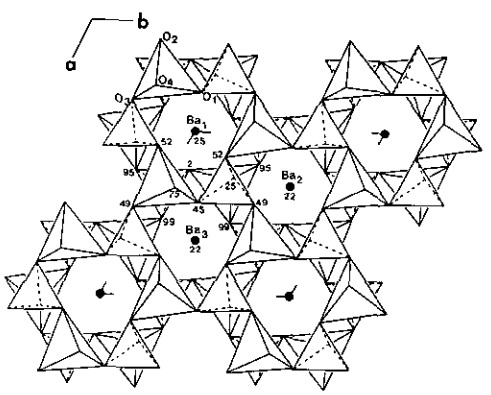

FIG. 3. Structure of $BaCoSiO_4$ viewed along the c axis. It consists of a Ba-stuffed tetrahedral framework derived from that of SiO_2 tridymite and similar to that of $KAlSiO_4$ kalsilite. The Co and Si atoms are fully ordered, with large CoO_4 tetrahedra pointing up and small SiO_4 tetrahedra pointing down. Atom heights are given in units of c/100. The structures of $BaMgSiO_4$ and $BaZnSiO_4$ are essentially identical.

148.6(5) for M = Mg, Zn, and Co, respectively. Interestingly, these Δz values and bond angles correlate very well with the trend observed for the c parameters of the hexagonal unit cells (cf. Table I), showing that the shorter c axis of the $BaCoSiO_4$ structure results from a more pronounced collapse of its tetrahedral framework. The origin of this greater collapse in the Co compound probably resides in the slightly larger difference between the Co–O (1.96 Å) and Si–O (1.63 Å) bond distances. Indeed, in the isostructural $BaZnGeO_4$ compound (*20*), the smaller tetrahedral bond length difference (Zn–O = 1.90 Å, Ge–O = 1.76 Å) is associated with a smaller degree of tetrahedral tilting [$\Delta z = 0.026$ between the O(1) and O(3) atoms].

Among the known tridymite derivative compounds containing barium, the silicates $BaMSiO_4$ discussed here and the germanate $BaZnGeO_4$ (*20*) are the only ones to crystallize with a $\sqrt{3} \times A$ superstructure of the kalsilite type. On the one hand, when the compounds contain larger atoms such as Ga and Fe in $BaGa_2O_4$ (*27*), $BaFe_2O_4$ (*28*), and $BaFe_{1.5}Al_{0.5}O_4$ (*29*), the topology of the tetrahedral framework becomes more complex and contains several kinds of six-membered rings with different sequences of tetrahedra pointing up and down. On the other hand, the compound $BaAl_2O_4$ (*8*), with a tetrahedral bond length ($< Al–O > = 1.76$ Å) intermediate between those of Co–O (1.96 Å) and Si–O (1.63 Å), adopts a kalsilite-like topology like $BaCoSiO_4$ but with a different superstructure, i.e., with a $(2 \times A, C)$ instead of a $(\sqrt{3} \times A, C)$ supercell. In $BaAl_2O_4$, the framework is built up of identical AlO_4 tetrahedra and is apparently able to accommodate the Ba atoms with only minor atom shifts and tetrahedral tilts. Overall, the known structures of the Ba-stuffed tridymite derivatives suggest that the formation of the $(\sqrt{3} \times A, C)$ kalsilite superstructure is favored for compounds containing tetrahedral atoms of sufficiently different sizes including small atoms, such as Si and Ge. Interestingly, the same superstructure is also found in othe isostructural silicates and germanates, such as the K-rich phases of the (K, Na)$AlGeO_4$ system (*15*) and the compound $(Na_{0.5}K_{0.5})GaSiO_4$, the structure of which has just been determined (*30*).

Acknowledgments

This work was supported by an operating grant to J. Barbier from the Natural Sciences and Engineering Research Council of Canada. The help of Dr. J. Britten with the data collection and structure refinement of $BaCoSiO_4$ is also acknowledged.

References

1. F. Liebau, "Structural Chemistry of Silicates," Springer-Verlag, Berlin/Heidelberg/New York/Tokyo (1985).
2. A. J. Perrotta and J. V. Smith, *Mineral. Mag.* **35,** 588 (1965).
3. W. A. Dollase and W. P. Freeborn, *Am. Mineral.* **62,** 336 (1977).
4. Y. Andou and A. Kawahara, *Mineral. J.* **11**(2), 72 (1982).
5. R. N. Abbott, *Am. Mineral.* **69,** 449 (1984).
6. A. Kawahara, Y. Andou, F. Marumo, and M. Okuno, *Mineral. J.* **13,** 260 (1987).
7. W. Hörkner and Hk. Müller-Buschbaum, *J. Inorg. Nucl. Chem.* **38,** 983 (1976).
8. W. Hörkner and Hk. Müller-Buschbaum, *Z. Anorg. Allg. Chem.* **451,** 40 (1979).
9. A. R. Schulze and Hk. Müller-Buschbaum, *Z. Anorg. Allg. Chem.* **475,** 205 (1981).
10. C. M. B. Henderson and D. Taylor, *Mineral. Mag.* **45,** 111 (1982).
11. D. Taylor, M. J. Dempsey, and C. M. B. Henderson, *Bull. Mineral.* **108,** 643 (1985).
12. J. Barbier and J. Neuhausen, *Eur. J. Mineral.* **2,** 273 (1990).
13. G. Lampert and R. Böhme, *Z. Kristallogr.* **176,** 29 (1986).
14. P. A. Sandomirskii, S. S. Meshalkin, I.V. Rozhdestvenskaya, L. N. Dem'yanets, and T. G. Uvarova, *Sov. Phys. Crystallogr.* **31**(5), 522 (1986).
15. J. Barbier and M. E. Fleet, *Phys. Chem. Minerals* **16,** 276 (1988).
16. J. Barbier and M. E. Fleet, *J. Solid State Chem.* **71,** 361 (1987).

17. P. C. Do Dinh and A. Durif, *Bull. Soc. Fr. Mineral. Cristallogr.* **87,** 108 (1964).
18. H. Takei, S. Tsunekawa, and M. Maeda, *J. Mater. Sci.* **15,** 2612 (1980).
19. H. Takei, *J. Appl. Crystallogr.* **13,** 400 (1980).
20. K. Iijima, F. Marumo, and H. Takei, *Acta Crystallogr. B* **38,** 1112 (1982).
21. Y. A. Malinovskii, *Sov. Phys. Dokl.* **29**(9), 706 (1984).
22. R. D. Shannon, *Acta Crystallogr. A* **32,** 751 (1976).
23. C. W. Tompson, D. F. R. Mildner, M. Mehregang, J. Sudol, R. Berliner, and W. B. Yelton, *J. Appl. Crystallogr.* **17,** 385 (1984).
24. V. F. Sears, Atomic Energy of Canada Limited, Report AECL-8490 (1984).
25. I. D. Brown and D. Altermatt, *Acta Crystallogr. B* **41,** 244 (1985).
26. S. Merlino, *in* "Feldspars and Feldspathoids" (W. L. Brown, Ed.), NATO ASI Series, C137, Reidel, Dordrecht.
27. H. J. Deiseroth and Hk. Müller-Buschbaum, *J. Inorg. Nucl. Chem.* **35,** 3177 (1973).
28. W. Leib and Hk. Müller-Buschbaum, *Z. Anorg. Allg. Chem.* **538,** 71 (1986).
29. M. Harder and Hk. Müller-Buschbaum, *Z. Anorg. Allg. Chem.* **448,** 135 (1979).
30. J. Barbier, B. Liu, and J. Weber, *Eur. J. Mineral.* in press, (1993).